



Mathematical Modeling of Oscillometric Blood Pressure Measurement: A Complete, Reduced Oscillogram Model

Vishaal Dhamotharan, *Graduate Student Member, IEEE*, Anand Chandrasekhar, Hao-Min Cheng, Chen-Huan Chen, Shih-Hsien Sung, Cederick Landry, Jin-Oh Hahn , *Senior Member, IEEE*, Aman Mahajan, Sanjeev G. Shroff, and Ramakrishna Mukkamala , *Senior Member, IEEE*

Abstract—Objective: Oscillogram modeling is a powerful tool for understanding and advancing popular oscillometric blood pressure (BP) measurement. A reduced oscillogram model relating cuff pressure oscillation amplitude (ΔO) to external cuff pressure of the artery (P_e) is: $\Delta O(P_e) = k \int_{P_d-P_e}^{P_s-P_e} g(P) dP$, where $g(P)$ is the arterial compliance versus transmural pressure (P) curve, P_s and P_d are systolic and diastolic BP, and k is the reciprocal of the cuff compliance. The objective was to determine an optimal functional form for the arterial compliance curve. **Methods:** Eight prospective, three-parameter functions of the brachial artery compliance curve were compared. The study data included oscillometric arm cuff pressure waveforms and invasive brachial BP from 122 patients covering a 20–120 mmHg pulse pressure range. The oscillogram measurements were constructed from the cuff pressure waveforms. Reduced oscillogram models, inputted with measured systolic and diastolic BP and each parametric brachial artery compliance curve function, were optimally fitted to the oscillogram measurements in the least squares sense. **Results:** An exponential-linear function yielded as good or better model fits compared to the other functions, with errors of 7.9 ± 0.3 and $5.1 \pm 0.2\%$ for tail-trimmed and lower half-trimmed oscillogram measurements. Importantly, this function was also the most tractable mathematically. **Conclusion:** A three-parameter exponential-linear function is an optimal form for the arterial compliance curve in the reduced oscillogram model and may thus serve as the standard function for this model henceforth. **Significance:** The complete, reduced oscillogram model determined herein can potentially improve oscillometric

BP measurement accuracy while advancing foundational knowledge.

Index Terms—Arterial compliance, blood pressure determination, cuffless blood pressure, derivative oscillometry, fixed ratios, mathematical model, oscillometry, parameter estimation.

I. INTRODUCTION

OSCILLOMETRY has emerged as the most important blood pressure (BP) measurement principle. Firstly, oscillometry in its conventional form of an automatic arm cuff device is now the most widely used BP monitoring method overall as well as in the hospital, office, home, and ambulatory setting [1]. Secondly, oscillometry may uniquely afford cuffless measurement of absolute BP using everyday devices [1], [2], [3].

The oscillometric principle exploits the sigmoidal blood volume-transmural pressure relationship of arteries (where transmural pressure = internal BP – external pressure of the artery.) The basic idea is to slowly vary the external pressure of the artery to first increase and then decrease the blood volume oscillation amplitude and thereafter apply an algorithm to the observed blood volume oscillation amplitude versus external pressure function (“oscillogram”) to compute BP. Conventional devices slowly inflate or deflate a cuff placed over the brachial artery to vary its external pressure, measure the pressure waveform inside the cuff to obtain both the external pressure via lowpass filtering and the variable-amplitude blood volume oscillations via highpass filtering, and apply population average algorithms to compute systolic/mean/diastolic BP from the oscillogram [4], [5], [6].

Mathematical modeling of oscillometric BP measurement is a powerful tool. Oscillogram models from reduced (accounting for only the crucial facets of the physiology, i.e., the sigmoidal relationship, which characterizes arterial stiffness, and BP) to complex (accounting for the detailed aspects of the physiology, e.g., the surrounding tissue and nonlinear cuff properties as well) have been developed [7], [8], [9], [10], [11], [12], [13], [14], [15], [16], [17], [18], [19], [20]. These models not only enhance understanding of the overall principle but also reveal the capabilities and limitations of the empirical BP computation algorithms (e.g., maximum amplitude [7], [8], [9], [10], [11],

Manuscript received 27 May 2022; revised 12 August 2022; accepted 17 August 2022. Date of publication 25 August 2022; date of current version 20 January 2023. This work was supported by the NIH under Grant HL146470. (Corresponding author: Ramakrishna Mukkamala.)

Vishaal Dhamotharan, Cederick Landry, and Sanjeev G. Shroff are with the Department of Bioengineering, University of Pittsburgh, USA.

Anand Chandrasekhar is with the Department of Electrical Engineering and Computer Science, MIT, USA.

Hao-Min Cheng, Chen-Huan Chen, and Shih-Hsien Sung are with the School of Medicine, National Yang Ming Chiao Tung University, Taiwan. Jin-Oh Hahn is with the Department of Mechanical Engineering, University of Maryland, USA.

Aman Mahajan is with the Departments of Bioengineering and Anesthesiology and Perioperative Medicine, University of Pittsburgh, USA.

Ramakrishna Mukkamala is with the Departments of Bioengineering and Anesthesiology and Perioperative Medicine, University of Pittsburgh, Pittsburgh, PA 15260 USA (e-mail: rmukkamala@pitt.edu).

Digital Object Identifier 10.1109/TBME.2022.3201433

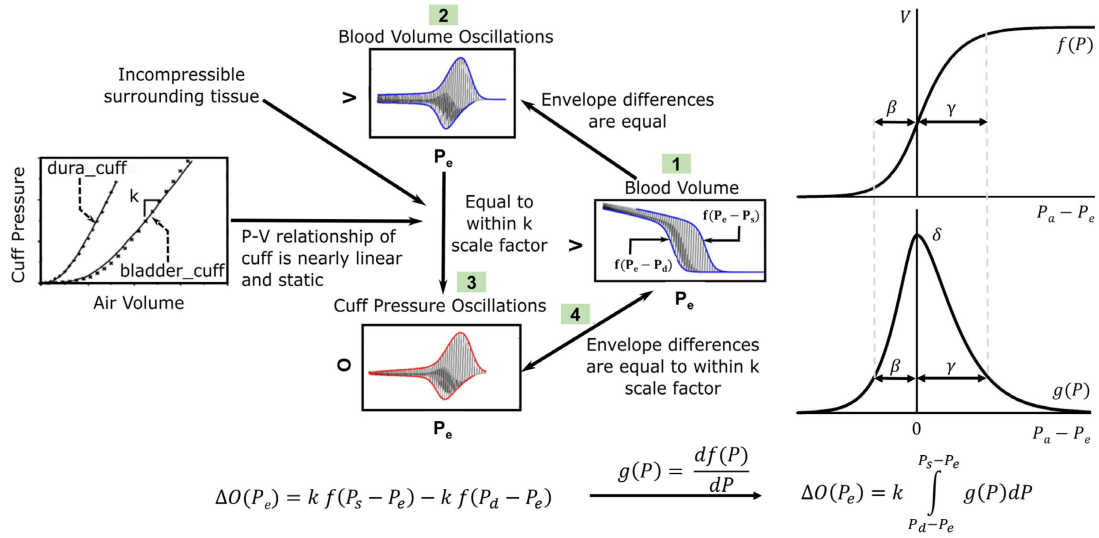


Fig. 1. Derivation of a useful, reduced oscillogram model with a typical arterial compliance curve. $\Delta O(P_e)$ is oscillogram for relating cuff pressure oscillation amplitude (ΔO ; difference in upper and lower red envelopes) to external cuff pressure of the artery (P_e); k , reciprocal of the cuff compliance for mapping blood volume to cuff pressure oscillations; $f(P)$, arterial blood volume (V)-transmural pressure (P) relationship; P_s and P_d , systolic and diastolic blood pressure (BP); and $g(P)$, arterial compliance curve. Adapted from [10].

[12], [13], [14], fixed ratios [8], [10], [12], [14], [15], [16], and derivative [10], [16]). Perhaps most interestingly, reduced models in particular can significantly improve the BP computation accuracy [16], [17], [18], [19], [20]. In contrast to complex models comprising many parameters, reduced models include only a few parameters denoting BP and defining the sigmoidal relationship, which may be uniquely estimated via optimal model fitting to the observed oscillogram. In this way, arterial stiffness is effectively measured along with BP for a patient-specific algorithm.

Fig. 1 schematically illustrates the derivation of a reduced oscillogram model [10], [19], [20]. This model relates cuff pressure oscillation amplitude (ΔO) to external cuff pressure of the artery (P_e) as follows:

$$\Delta O(P_e) = k f(P_s - P_e) - k f(P_d - P_e), \quad (1)$$

where $f(P)$ is the sigmoidal blood volume-transmural pressure (P) relationship, k is the reciprocal of the cuff compliance for mapping blood volume to cuff pressure oscillations, and P_s and P_d are systolic and diastolic BP. The model may be re-expressed as follows:

$$\Delta O(P_e) = k \int_{P_d-P_e}^{P_s-P_e} g(P) dP, \quad (2)$$

where $g(P)$ is the derivative of $f(P)$ with respect to P and denotes the arterial compliance versus transmural pressure curve. The $g(P)$ curve is known to be unimodal and right skewed with a peak near zero transmural pressure (see Fig. 1) [12], and several different parametric functions have been used to parsimoniously define the curve [9], [10], [11], [12], [13], [14], [15], [16], [17], [18], [19], [20]. However, the best amongst these and other possible functions remains unknown. As a result, the reduced oscillogram model is incomplete in the sense that it is missing a standard function to parameterize the arterial compliance curve $g(P)$.

We performed a systematic investigation using extensive and high-fidelity patient data to establish a best parametric function for defining the brachial artery compliance curve in the reduced oscillogram model. We found that a little utilized three-parameter exponential-linear function is an optimal formulation that can serve as a standard to complete the model.

II. METHODS

We studied oscillometric arm cuff pressure waveforms and accurate brachial BP measurements from many patients covering a wide BP range that were collected under IRB approval. We selected prospective parametric functions to define the brachial artery compliance curve according to predefined criteria. We analyzed the data to compare the parametric functions in terms of fitting the reduced oscillogram model to the experimentally measured oscillograms.

A. Patient Data

We used existing, de-identified patient data for this investigation. The data and IRB-approved study procedures are described in detail elsewhere [20], [21], [22]. Briefly, the data included 128 cardiac catheterization patients and 19 healthy patients. The cardiac catheterization patient data typically comprised two oscillometric cuff pressure waveforms via repeated fast inflation-slow deflation-constant cuff pressure cycles of an arm cuff device (WatchBP Office, Microlife AG, Switzerland or VP-1000, Omron Colin, Japan) and simultaneous measurement of the gold standard brachial BP waveform via a micromanometer-tipped catheter (SPC-320, Millar Instruments, USA) in the opposite arm. The waveforms were available at baseline conditions and after administration of sublingual nitroglycerin (NTG) to

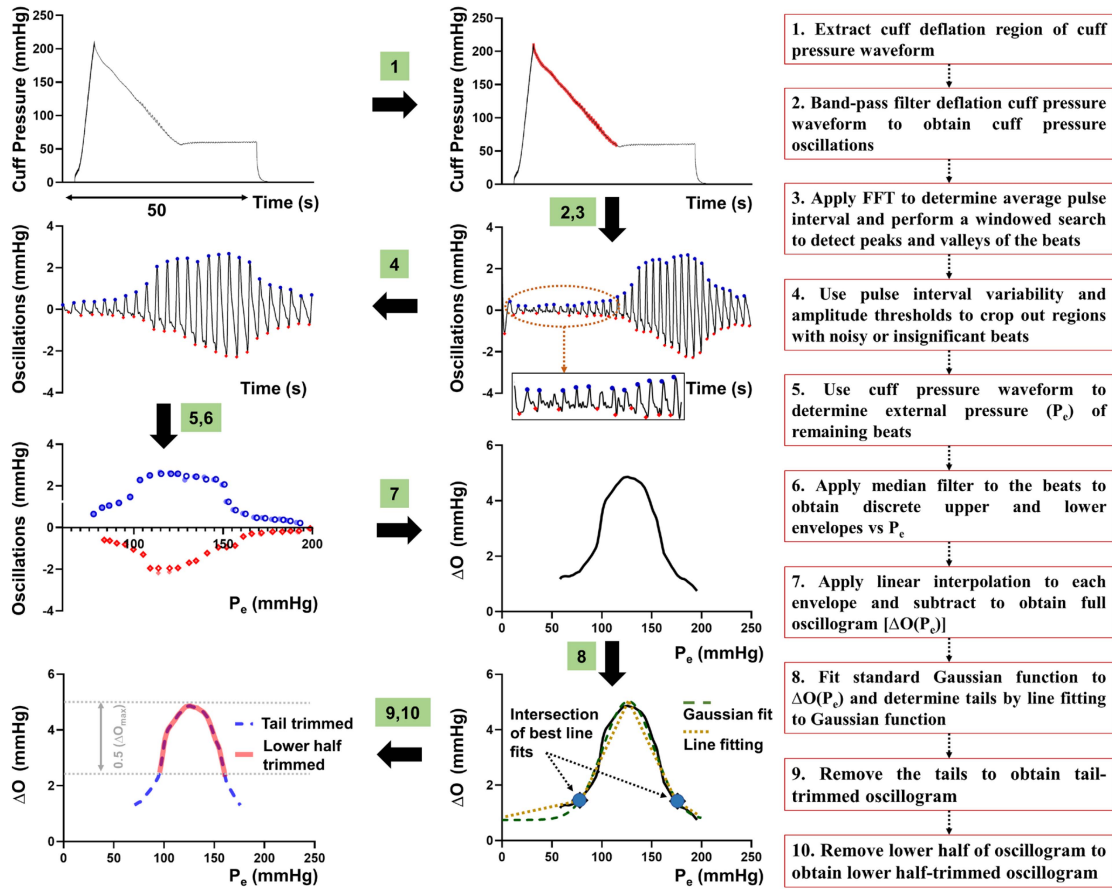


Fig. 2. Flow chart of an algorithm for constructing the oscillogram measurement from the cuff pressure waveform. The cuff pressure waveform obtained during fast cuff inflation followed by slow cuff deflation and then constant cuff pressure at 60 mmHg is automatically analyzed to construct tail-trimmed and lower half-trimmed oscillogram measurements. Important user-selected variables: Band-pass filter of 6th order with cut-off frequencies of 0.75 and 4 Hz (step 2); amplitude thresholds < 0.2 mmHg for peaks and > -0.1 mmHg for valleys and pulse interval variability $< 0.65/PR$ and $> 1.35/PR$, where PR is FFT-based pulse rate (steps 3 and 4); and median filter of 6th order (Step 6).

reduce BP in a subset of the patients (see Results for numbers). The healthy patient data included similar oscillometric cuff pressure waveforms and simultaneous measurement of clinical standard brachial BP via manual auscultation performed on the same arm. The sampling rate of all waveforms was 250 Hz.

We screened the cuff pressure and BP waveforms to exclude unreliable data. We used the following criteria for data exclusion: (1) inter-arm cuff BP differences (which were assessed prior to data collection for the cardiac catheterization patients) of >10 mmHg; (2) substantial cuff pressure waveform artifact (e.g., due to motion); (3) insufficient cuff pressure range to form a full oscillogram with inverted U-shape; and (4) unsteady brachial BP waveform. We also eliminated all waveforms with significant arrhythmias likewise based on visual inspection.

B. Prospective Parametric Brachial Artery Compliance Curve Functions

We used the following criteria for selecting prospective parametric functions to define the brachial artery compliance curve

$g(P)$: (1) unimodal and (2) right-skewable with (3) three parameters controlling the peak amplitude and negative and positive transmural pressure widths of the curve (see Fig. 1). We prioritized published functions. Table I lists the eight parametric functions that we selected. We identified the first five functions from previous studies: Exponential (EX) [9], [10], [11], [14], [16], [17], Drzewiecki (DZ) [12], [15], [18], Gaussian (GA) [10], Exponential-Linear (EL) [10], and Fisk (FS) [19], [20]. We identified the last three functions from a compendium of probability density functions: Weibull (WB), Burr (BR), and Inverse Burr (IB) [23].

C. Data Analysis

We first constructed the “oscillogram measurements” from the cuff pressure waveforms via an automated algorithm. Fig. 2 shows a detailed flowchart of this algorithm.

We then optimally fitted the reduced oscillogram model of (2) with each parametric brachial artery compliance curve function to the oscillogram measurements in the least squares sense. We set P_s and P_d in each of the models to the measured brachial BP values (i.e., average SP and DP of the invasive BP waveform

TABLE I
PROSPECTIVE PARAMETRIC FUNCTIONS FOR DEFINING THE BRACHIAL ARTERY COMPLIANCE CURVE IN THE REDUCED OSCILLOGRAM MODEL ($g(P)$ IN (2))

Exponential (EX) [9], [10], [11], [14] [16], [17]	$de^{\frac{P}{b}} u(-P) + de^{-\frac{P}{c}} u(P)$
Drzewiecki (DZ) [12], [15], [18]	$d \left[\left(\frac{h}{(hP+b)(1+e^{-cP})} \right) + \left(\frac{ce^{-cP} \ln(hP+b)}{(1+e^{-cP})^2} \right) \right]$
Gaussian (GA) [10]	$de^{-(\frac{P}{b})^2} u(-P) + de^{-(\frac{P}{c})^2} u(P)$
Exponential-Linear (EL) [10]	$de^{\frac{P}{b}} \left(-\frac{P}{b} + 1 \right) u(-P) + de^{-\frac{P}{c}} \left(\frac{P}{c} + 1 \right) u(P)$
Fisk (FS) [19], [20]	$\frac{dc}{b} \left(\frac{P}{b} + \sqrt{\frac{c-1}{c+1}} \right)^{c-1} \left[1 + \left(\frac{P}{b} + \sqrt{\frac{c-1}{c+1}} \right)^{c-2} \right]$
Weibull (WB) [proposed]	$\frac{dc}{b} \left(\frac{P}{b} + \sqrt{\frac{c-1}{c}} \right)^{c-1} \exp \left[- \left(\frac{P}{b} + \sqrt{\frac{c-1}{c}} \right)^c \right]$
Burr (BR) [proposed]	$\frac{dc}{b} \left(\frac{P}{b} + \sqrt{\frac{c-1}{2c+1}} \right)^{c-1} \left[1 + \left(\frac{P}{b} + \sqrt{\frac{c-1}{2c+1}} \right)^{c-3} \right]$
Inverse Burr (IB) [proposed]	$\frac{dc}{b} \left(\frac{P}{b} + \sqrt{\frac{c-1}{c+1}} \right)^{-c-1} \left[1 + \left(\frac{P}{b} + \sqrt{\frac{c-1}{c+1}} \right)^{-c-2} \right]$

b, c, d are parameters specifying the peak amplitude (δ), left transmural pressure width (β), and right transmural pressure width (γ) of the unimodal and right-skewed $g(P)$ (see Fig. 1). $u(\cdot)$ is the unit-step function (with $u(0) = 0.5$). h is set so that the function peaks at $P = 0$ and therefore contains only three unknown parameters.

over the time duration of the oscillogram or auscultation SP and DP) and combined the d parameter of each function with the reciprocal of the cuff compliance parameter (i.e., $a = d \cdot k$). In preliminary analyses, we also explored the impact of the peak location of the functions and found that it did not have any significant influence on the fitting (e.g., <5% model fitting error difference for peak locations between -5 and 5 mmHg). The reason was that the other function parameters were able to compensate (i.e., the negative/positive transmural pressure curve widths increased/decreased as the peak location increased). We therefore maintained the peak location at 0 mmHg as indicated in Table I and in line with other data and the transition from bending to tensile mechanics [12], [24]. Hence, we specifically performed three-parameter, quadratic minimizations to fit the models as follows:

$$\min_{\{a,b,c\}} \int_{P_{e,min}}^{P_{e,max}} \left(\Delta O(P_e) - a \int_{P_d-P_e}^{P_s-P_e} g(P, b, c) dP \right)^2 dP_e \quad (3)$$

We solved the optimization problems using an exhaustive search over empirically established ranges for the three unknown parameters of each function. We fitted the models over different cuff pressure ranges (i.e., $[P_{e,min}, P_{e,max}]$): (1) tail-trimmed and (2) lower half-trimmed. The purpose of the tail-trimmed range was to eliminate the flat tails that appeared on both

ends of many oscillograms and are likely due to phenomena not accounted for by the reduced model (e.g., pulsations from lower-pressure vessels under the cuff and from arteries proximal to the cuff). The purpose of the lower half-trimmed range (i.e., oscillogram portion with amplitude >50% of the maximal amplitude) was to investigate the model fitting over the main portion of the oscillogram. Fig. 2 also illustrates the tail- and lower half-trimming component of the oscillogram measurement construction algorithm.

We evaluated each parametric function in terms of the normalized-root-mean-squared-error (NRMSE) of each model fit in units of %. The NRMSE was defined as follows

$$NRMSE = 100$$

$$\cdot \sqrt{\frac{\int_{P_{e,min}}^{P_{e,max}} \left(\Delta O(P_e) - \hat{a} \int_{P_d-P_e}^{P_s-P_e} g(P, \hat{b}, \hat{c}) dP \right)^2 dP_e}{\int_{P_{e,min}}^{P_{e,max}} (\Delta O(P_e))^2 dP_e}}, \quad (4)$$

where hat ($\hat{\cdot}$) indicates the optimal parameter estimates via (3). The R^2 value and other evaluation metrics did not reveal further insights. We statistically compared the NRMSEs of the eight functions using Dunnett's test, with the parametric function yielding the lowest average NRMSE over the measurements as the reference. Prior to statistical analyses, we averaged the NRMSEs of multiple measurements per patient to ensure independence of samples. We also analogously performed subgroup analysis to further compare the top performing functions. In addition, we analyzed the model fits in several other ways including detailed visual inspections to provide representative examples of the overall capabilities and limitations of the functions in oscillogram model fitting. We lastly invoked physiology and paired t-tests to assess the top performing functions in terms of their parameter estimates.

III. RESULTS

The final patient data for analysis included 215 reliable oscillogram arm cuff pressure waveform-brachial BP measurement pairs from 122 patients (58 ± 15 years old, 73% male, 163 ± 8 cm, 69 ± 14 kg). These data included 132 and 83 measurement pairs during baseline and NTG conditions, respectively. The BP ranges were 90-190 mmHg for systolic BP (SP), 58-96 mmHg for diastolic BP (DP), and 20-120 mmHg for pulse pressure (PP).

Fig. 3(a) and (b) show the NRMSEs (mean \pm SE) of the fits of the reduced oscillogram models with each of the eight parametric brachial artery compliance curve functions (see Table I) to the tail-trimmed and lower half-trimmed oscillogram measurements, respectively. The functions are listed in order from best (lowest mean NRMSE) to worst (highest mean NRMSE), and an asterisk indicates that a function yielded an NRMSE that was statistically higher than that via the best function by at least 5% (which we considered to be of practical significance). For the tail-trimmed oscillogram measurements, the GA function performed best with an NRMSE of $7.6 \pm 0.3\%$, while the EL and WB functions produced similar NRMSEs of 7.9 ± 0.3 and $8.0 \pm 0.3\%$. The EX function provided a higher but still relatively

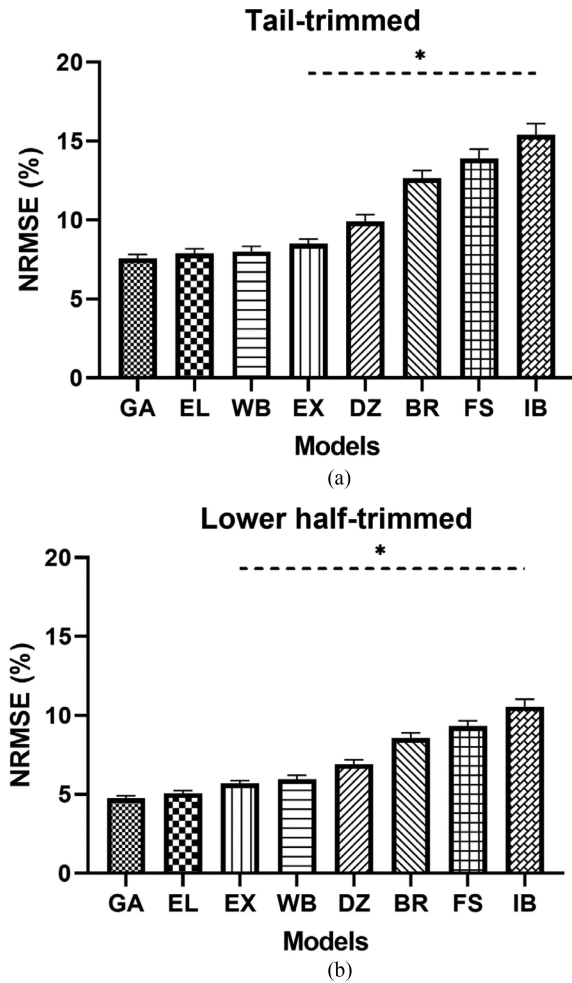


Fig. 3. Normalized-root-mean-squared-errors (NRMSEs (mean \pm SE); $N = 122$) of the fits of the reduced oscillogram models with each parametric brachial artery compliance curve function (see Table I) to the (a) tail-trimmed and (b) lower half-trimmed oscillogram measurements. * indicates that the function yielded an NRMSE that was statistically higher than the NRMSE of the left-most function (which produced the lowest mean NRMSE) by at least 5% via Dunnett's test.

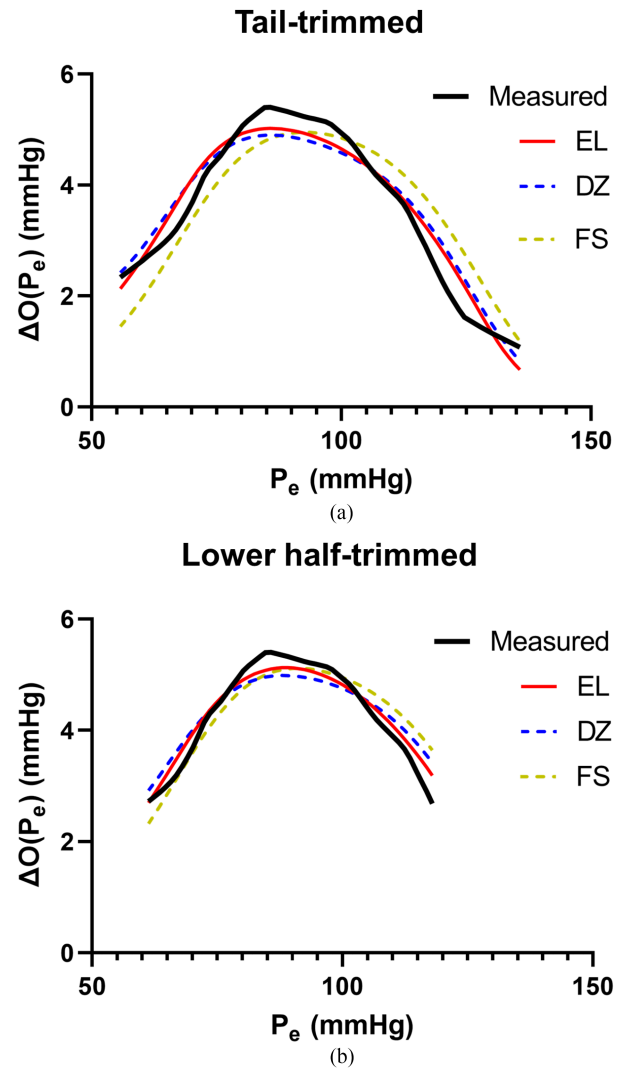


Fig. 4. Representative examples of model fits to the (a) tail-trimmed and (b) lower half-trimmed oscillogram measurements. In these particular examples, the EL, DZ, and FS functions yielded NRMSEs of 7.9 and 5.4, 9.7 and 7.3, 15.3 and 8.3%, respectively.

close NRMSE of $8.5 \pm 0.3\%$. The remaining four functions resulted in noticeably higher NRMSEs from $9.9 \pm 0.4\%$ for the DZ function to $15.4 \pm 0.7\%$ for the IB function. For the lower half-trimmed oscillogram measurements, all functions yielded lower NRMSEs as expected. The relative performance of the functions was almost the same as for the tail-trimmed oscillogram measurements, with the GA and EL functions producing the lowest and similar NRMSEs of 4.8 ± 0.2 and $5.1 \pm 0.2\%$.

Fig. 4(a) and (b) illustrate representative examples of relatively good (EL function), moderate (DZ function), and poor (FS function) model fits to the tail-trimmed and lower half-trimmed oscillogram measurements, respectively. For the tail-trimmed oscillogram measurements, as shown and on average, the EL function resulted in slight underestimation and overestimation of the main and lower portions of the oscillogram, respectively (by a few percent of the oscillogram peak amplitude). For the lower half-trimmed oscillogram measurements, as shown, the EL function again resulted in systematic underestimation of the oscillogram peak but to an even slighter extent than for the

tail-trimmed oscillograms. Such systematic fitting errors were likewise evident for the GA, WB, and EX functions.

Fig. 5 shows the NRMSEs of the fits of the reduced oscillogram model with the GA, EL, WB, and EX functions to the tail-trimmed oscillogram measurements for the following subgroups: age of <60 and ≥ 60 years (a), males and females (b), baseline and NTG conditions (c), and PP of <60 and ≥ 60 mmHg (d). The plots are illustrated analogously to Fig. 3, but the results for the lower half-trimmed oscillogram measurements, which do not provide further insights as mentioned above, are not included. The GA function yielded the lowest NRMSEs across the eight subgroups from 6.4 ± 0.5 to $8.0 \pm 0.3\%$, while the EL and WB functions produced similar NRMSEs. The EX function provided higher NRMSEs for four of the subgroups. Another observation is that the four functions generally provided relatively better fits for normal PP than high PP and for females than males. High PP has typically been problematic in oscillometry.

Fig. 6 shows the parameter estimates of the EL function resulting from model fitting to the tail-trimmed oscillogram

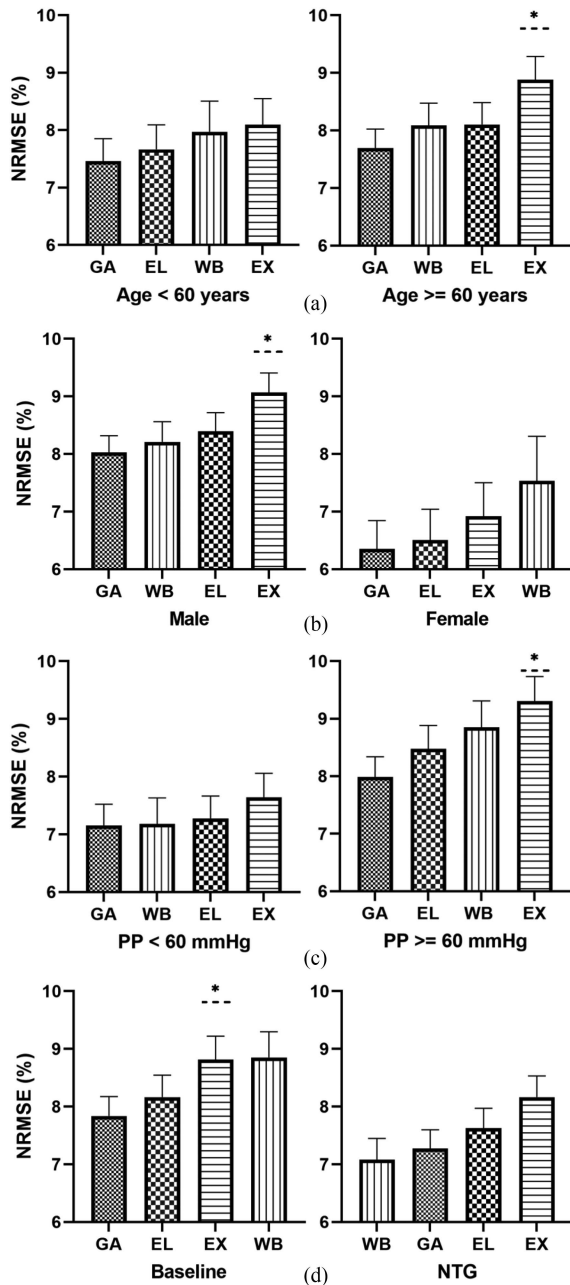


Fig. 5. NRMSEs (mean \pm SE) of the fits of the reduced oscillogram models with the top-performing parametric brachial artery compliance curve functions to the tail-trimmed oscillogram measurements for different subgroups. (a) <60 years old ($N = 61$) and ≥ 60 years old ($N = 61$), (b) males ($N = 89$) and females ($N = 33$), (c) baseline ($N = 98$) and nitroglycerin (NTG, $N = 64$), and (d) <60 mmHg pulse pressure (PP, $N = 60$) and ≥ 60 mmHg PP ($N = 62$). * indicates that the function yielded an NRMSE that was statistically higher than the NRMSE of the left-most function (which produced the lowest mean NRMSE) by at least 5% via Dunnett's test.

measurements. The c parameter was significantly greater than the b parameter overall (see Fig. 6(a)), which is consistent with a right-skewed, arterial compliance curve. The c parameter also significantly increased after NTG administration (see Fig. 6(b)), which is congruent with the vasorelaxation effect of the drug. The parameter estimates of the GA and EX functions (but not the WB function) were equally predictive of known physiology

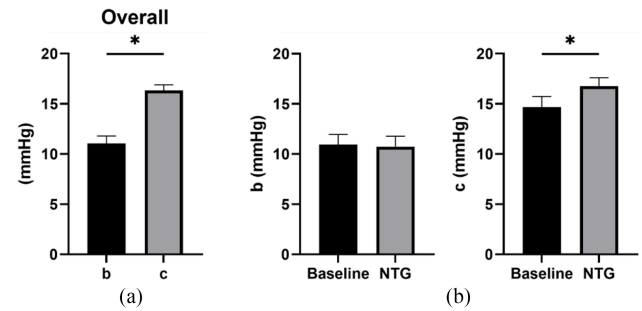


Fig. 6. The b and c parameter estimates for the EL function (a) overall ($N = 122$) and (b) before and after NTG ($N = 39$). The estimates were obtained via model fitting to the tail-trimmed oscillogram measurements. * indicates significant difference via paired t-tests. The parameter estimates for the GA and EX functions showed similar trends.

and thus not shown. Hence, the parameter estimates of the EL, GA, and EX functions also made sense to a similar extent.

IV. DISCUSSION

Reduced oscillogram modeling is a powerful tool for understanding and advancing popular oscillometric BP measurement. A reduced oscillogram model is known to be a running integral of the unimodal arterial compliance curve over the external pressure of the artery, with parameters denoting the peak amplitude of the curve at zero transmural pressure, the negative and positive transmural pressure widths of the curve, and SP and DP (see Fig. 1). However, an optimal functional form of the arterial compliance curve has not been identified. We compared five, three-parameter functions of the brachial artery compliance curve that have been employed in published oscillogram models [9], [10], [11], [12], [14], [15], [16], [17], [18], [19], [20] and three additional prospective three-parameter functions that we identified according to predefined criteria (see Table I) in terms of their ability to fit oscillogram measurements as well as to produce physiological parameter estimates. We conducted a systematic investigation using patient data comprising simultaneous measurements of oscillometric arm cuff pressure waveforms and invasive (mainly) or auscultatory brachial SP and DP from many patients ($N = 122$) covering a wide BP range (e.g., 20 to 120 mmHg PP range). We constructed the oscillogram measurements from the oscillometric cuff pressure waveforms (see Fig. 2) and performed least squares fitting of the reduced oscillogram model, inputted with the measured brachial SP and DP and each parametric function, to the oscillogram measurements.

We found that the GA and EL functions yielded the best and similar oscillogram model fits (see Figs. 3 and 5). The WB function closely followed in the fitting with the EX function not that far behind (see Figs. 3 and 5). The DZ, FS, BR, and IB functions produced noticeably poorer fits (see Figs. 3 and 4). The four top performing functions did result in slight, systematic underestimation of the main portion of the oscillogram and slight, systematic overestimation of its tails (see Fig. 4). Potential sources of the model fitting error for these four functions include respiration, compressibility of surrounding tissue, and

nonlinearity of the cuff (see Figs. 1 and 2). The GA, EL, and EX functions also produced parameter estimates with similar capacity in predicting the known right-skewed brachial artery compliance curve and the known vasorelaxation effect of NTG (see Fig. 6).

Our findings here are rather unexpected. The DZ function, which is based on direct fitting to arterial compliance data (i.e., arterial cross-sectional area and pressure measurements) [12], [24] and has been used in several studies [12], [15], [18], and the FS function, which we utilized previously to show the significant added value of a patient-specific oscillometric BP computation algorithm [19], [20], did not fare well compared to other functions. The FS function, in fact, yielded model fits with almost twice the error as other functions. The EX function, which has been used in the most previous studies [9], [10], [11], [14], [16], [17], performed well but not at the level of other functions. On the other hand, the WB function, which we proposed for this study, produced relatively good fitting, while the EL function, which we introduced recently [10], performed at least as well as any of the prospective functions in every considered case.

Amongst the prospective functions, the EL function stands out in terms of mathematical convenience. In contrast to the GA function, it may be integrated so as to yield a closed-form expression for the reduced oscillogram model of (2) and thus insightful analytical expressions [10]. Unlike the EX function, it is twice differentiable and thus amenable to fast, derivative-based methods for oscillogram model fitting. Use of fast methods would be important for patient-specific oscillometric BP computation algorithms, which require the estimation of five parameters including systolic and diastolic BP. In contrast to the WB, DZ, FS, BR, and IB functions, the parameters of the EL function have one-to-one correspondence to the peak amplitude ($d = \delta$), negative transmural pressure width ($b = \beta$), and positive transmural pressure width ($c = \gamma$) of the arterial compliance curve (see Fig. 1). Such one-to-one correspondence would simplify the interpretation of any model-based result.

In sum, the EL function afforded as good or better oscillogram model fitting compared to the other seven prospective functions and is most tractable mathematically. In this sense, the EL function is best for the reduced oscillogram model. Substituting the EL function in the fourth row of Table I for $g(P)$ in (2) and then integrating gives a complete, reduced oscillogram model relating cuff pressure oscillation amplitude (ΔO) to external cuff pressure of the brachial artery (P_e) as follows:

$$\begin{aligned} \Delta O(P_e) = & a \left((P_d - P_e + 2c) e^{-\frac{P_d - P_e}{c}} \right. \\ & \left. - (P_s - P_e + 2c) e^{-\frac{P_s - P_e}{c}} \right) u(P_d - P_e) \\ & + a \left(2(b + c) + (P_d - P_e - 2b) e^{\frac{P_d - P_e}{b}} \right. \\ & \left. - (P_s - P_e + 2c) e^{-\frac{P_s - P_e}{c}} \right) (u(P_e - P_d) \\ & - u(P_e - P_s)) + a \left((P_d - P_e - 2b) e^{\frac{P_d - P_e}{b}} \right. \\ & \left. - (P_s - P_e - 2b) e^{\frac{P_s - P_e}{b}} \right) u(P_e - P_s), \quad (5) \end{aligned}$$

where P_s and P_d are SP and DP; a is the ratio of the peak amplitude of the brachial artery compliance curve to the cuff compliance; b and c are the negative and positive transmural pressure widths of the arterial compliance curve; and $u(\cdot)$ is the unit-step function.

Interestingly, we recently showed that the cuff (external) pressure at maximum oscillogram amplitude ($P_e^{\Delta O_{max}}$) corresponds to a weighted average of SP and DP, where the weightings are in terms of b and c parameters of the EL function [10]. Using the overall average b and c parameter estimates from the current much larger patient study (see Fig. 6(a)) gives more accurate weightings as follows: $P_e^{\Delta O_{max}} = 0.41P_s + 0.59P_d$. This $P_e^{\Delta O_{max}}$ formula is remarkably similar to the following standard formula for computing mean BP (P_m , i.e., the time average of the BP waveform) from SP and DP: $P_m = 0.4P_s + 0.6P_d$ [25]. This coincidence may partly explain why $P_e^{\Delta O_{max}}$ has long been believed to indicate mean BP. However, the P_m formula breaks down for high PP and other conditions, and, as we showed earlier, $P_e^{\Delta O_{max}}$ agrees significantly better to a weighted average of SP and DP than mean BP over a wide hemodynamic range.

It is worth reiterating that the purpose of this study was to establish an optimal parametric function to characterize the brachial artery compliance curve for a reduced oscillogram model. The oscillogram is essentially a smoothed version of the arterial compliance curve (as indicated by (2)). If we had determined the parametric function by direct fitting to arterial compliance curve data, we would have likely found another function (e.g., DZ function) and obtained differing results overall (e.g., greater variation in the GA, EL, and EX model fits). The best function for oscillogram model fitting (i.e., GA or EL function) may be able to represent the arterial compliance curve and mitigate systematic modeling error.

It should also be mentioned that the present study does not indicate that a patient-specific oscillometric BP computation algorithm using the previous FS function [19], [20] or any other of the seven functions could not perform better than a population average algorithm, especially when the patient-specific algorithm is optimized for the function (in terms of, e.g., parameter and cuff pressure fitting ranges). This study instead suggests that a patient-specific algorithm using the EL function in particular could perform better than when using the FS or other functions. Extending the patient-specific algorithm with the EL function is surely a worthy future research direction.

While we strived to conduct a thorough investigation, we have not proved that the EL function yields the best possible oscillogram fitting in the least squares sense. However, the small systemic fitting errors produced by this function suggest that other prospective functions could only add marginal value. Although our extensive and high-fidelity patient data were a major strength, our findings may not extend to measurement sites beyond the brachial artery (arm) such as the radial (wrist), dorsal pedal (ankle), digital (finger), and transverse palmar arch (fingertip) arteries. Our results may also not be applicable to photoplethysmography measurements of blood volume oscillations or variation in external pressure of the artery via non-pneumatic means [1], [2], [3]. It is additionally unclear if our findings translate to populations not represented by our patient data

including very obese people and patients with diastolic hypertension. However, in absence of further analyses and data, it may be rational to use the EL function in the reduced oscillogram model under broad circumstances.

V. CONCLUSION

We performed a systematic investigation of extensive and high-fidelity patient data to find that a little utilized three-parameter exponential-linear (EL) function is an optimal form for the arterial compliance curve in a reduced oscillogram model. Future studies on oscillometry can now employ the proven EL function in contrast to earlier studies, which, according to the findings herein, utilized suboptimal [9], [10], [11], [14], [16], [17] or even relatively poorly performing functions [12], [15], [18], [19], [20]. Furthermore, subsequent, exclusive use of the substantiated EL function would facilitate comparisons (of, e.g., parameter estimates) across different studies. In sum, the EL function could serve as the standard form of the arterial compliance curve in the reduced oscillogram model henceforth. This complete model could guide or complement investigations on oscillometry – the most important BP measurement principle.

REFERENCES

- [1] R. Mukkamala, G. S. Stergiou, and A. P. Avolio, "Cuffless blood pressure measurement," *Annu. Rev. Biomed. Eng.*, vol. 24, pp. 203–230, 2022, doi: [10.1146/annurev-bioeng-110220](#).
- [2] A. Chandrasekhar et al., "An iPhone application for blood pressure monitoring via the oscillometric finger pressing method," *Sci. Rep.*, vol. 8, no. 1, pp. 1–6, Dec. 2018, doi: [10.1038/s41598-018-31632-x](#).
- [3] A. Chandrasekhar et al., "Smartphone-based blood pressure monitoring via the oscillometric finger-pressing method," *Sci. Transl. Med.*, vol. 10, no. 431, 2018, Art. no. eaap8674, doi: [10.1126/scitranslmed.aap8674](#).
- [4] B. S. Alpert, D. Quinn, and D. Gallick, "Oscillometric blood pressure: A review for clinicians," *J. Amer. Soc. Hypertension*, vol. 8, no. 12, pp. 930–938, 2014, doi: [10.1016/j.jash.2014.08.014](#).
- [5] G. A. van Montfrans, "Oscillometric blood pressure measurement: Progress and problems," *Blood Press. Monit.*, vol. 6, no. 6, pp. 287–290, 2001, doi: [10.1097/00126097-200112000-00004](#).
- [6] T. G. Pickering et al., "Recommendations for blood pressure measurement in humans and experimental animals," *Circulation*, vol. 111, no. 5, pp. 697–716, Feb. 2005, doi: [10.1161/01.CIR.0000154900.76284.F6](#).
- [7] G. W. Mauck et al., "The meaning of the point of maximum oscillations in cuff pressure in the indirect measurement of blood pressure—part II," *J. Biomechanical Eng.*, vol. 102, no. 1, pp. 28–33, 1980, doi: [10.1115/1.3138195](#).
- [8] M. Ursino and C. Cristalli, "A mathematical study of some biomechanical factors affecting the oscillometric blood pressure measurement," *IEEE Trans. Biomed. Eng.*, vol. 43, no. 8, pp. 761–778, Aug. 1996, doi: [10.1109/10.508540](#).
- [9] P. D. Baker, D. R. Westenskow, and K. Kück, "Theoretical analysis of non-invasive oscillometric maximum amplitude algorithm for estimating mean blood pressure," *Med. Biol. Eng. Comput.*, vol. 35, no. 3, pp. 271–278, 1997, doi: [10.1007/bf02530049](#).
- [10] A. Chandrasekhar et al., "Formulas to explain popular oscillometric blood pressure estimation algorithms," *Front. Physiol.*, vol. 10, Nov. 2019, Art. no. 1415, doi: [10.3389/fphys.2019.01415](#).
- [11] R. Raamat et al., "Mathematical modelling of non-invasive oscillometric finger mean blood pressure measurement by maximum oscillation criterion," *Med. Biol. Eng. Comput.*, vol. 37, no. 6, pp. 784–788, 1999, doi: [10.1007/BF02513382](#).
- [12] G. Drzewiecki, R. Hood, and H. Applet, "Theory of the oscillometric maximum and the systolic and diastolic detection ratios," *Ann. Biomed. Eng.*, vol. 22, pp. 88–96, 1994, doi: [10.1114/1.130](#).
- [13] R. Raamat et al., "Errors of oscillometric blood pressure measurement as predicted by simulation," *Blood Press. Monit.*, vol. 16, no. 5, pp. 238–245, Oct. 2011, doi: [10.1097/MBP.0b013e32834af752](#).
- [14] F. K. Forster and D. Turney, "Oscillometry determination of diastolic, mean and systolic blood pressure—A numerical model," *J. Biomechanical Eng.*, vol. 108, no. 4, pp. 359–364, 1986, doi: [10.1115/1.3138629](#).
- [15] J. Liu, J. O. Hahn, and R. Mukkamala, "Error mechanisms of the oscillometric fixed-ratio blood pressure measurement method," *Ann. Biomed. Eng.*, vol. 41, no. 3, pp. 587–597, Mar. 2013, doi: [10.1007/s10439-012-0700-7](#).
- [16] C. F. Babb, "Oscillometric measurement of systolic and diastolic blood pressures validated in a physiologic mathematical model," *Biomed. Eng. Online*, vol. 11, pp. 1–22, Aug. 2012, doi: [10.1186/1475-925X-11-56](#).
- [17] J. S. Clark and S. Sun, "Total compliance method and apparatus for noninvasive arterial blood pressure measurement," U.S. Patent 5423322A, Jun. 13, 1995.
- [18] M. Forouzanfar et al., "Mathematical modeling and parameter estimation of blood pressure oscillometric waveform," in *Proc. IEEE Symp. Med. Meas. Appl., Proc.*, 2012, pp. 208–213, doi: [10.1109/MeMeA.2012.6226639](#).
- [19] J. Liu et al., "Patient-specific oscillometric blood pressure measurement," *IEEE Trans. Biomed. Eng.*, vol. 63, no. 6, pp. 1220–1228, Jun. 2016, doi: [10.1109/TBME.2015.2491270](#).
- [20] J. Liu et al., "Patient-specific oscillometric blood pressure measurement: Validation for accuracy and repeatability," *IEEE J. Transl. Eng. Health Med.*, vol. 5, 2017, Art. no. 1900110, doi: [10.1109/JTEHM.2016.2639481](#).
- [21] H. M. Cheng et al., "Measurement of central aortic pulse pressure: Noninvasive brachial cuff-based estimation by a transfer function vs. a novel pulse wave analysis method," *Amer. J. Hypertension*, vol. 25, no. 11, pp. 1162–1169, Nov. 2012, doi: [10.1038/ajh.2012.116](#).
- [22] H. M. Cheng et al., "Measurement accuracy of a stand-alone oscillometric central blood pressure monitor: A validation report for Microlife WatchBP office central," *Amer. J. Hypertension*, vol. 26, no. 1, pp. 42–50, Jan. 2013, doi: [10.1093/ajh/hps021](#).
- [23] M. P. McLaughlin, "Compendium of common probability distributions," 2nd Edition, v2.7, 2016.
- [24] G. Drzewiecki and J. J. Pilla, "Noninvasive measurement of the human brachial artery pressure-area relation in collapse and hypertension," *Ann. Biomed. Eng.*, vol. 26, no. 6, pp. 965–974, 1998, doi: [10.1007/BF02368225](#).
- [25] W. J. W. Bos et al., "How to assess mean blood pressure properly at the brachial artery level," *J. Hypertension*, vol. 25, no. 4, pp. 751–755, 2007. [Online]. Available: <http://journals.lww.com/jhypertension>